JURNAL KIMIA VALENSI
p-ISSN: 2460-6065; e-ISSN: 2548-3013
Journal homepage: https://journal.uinjkt.ac.id/index.php/valensi
Research Article

Synthesis, Characterization, Molecular Docking Studies and Pharmaceutical Evaluation of Some Novel [1,2,4]Triazolo[3,4-*B*][1,3,4]Thiadiazole

Athraa Hameed Mekky[1*], Fadil M. Hamed[2], Bassam A. Hassan[3]

[1]*Department of Chemistry, College of Science, University of Thi-Qar, Thi-Qar, 64001, Iraq*
[2]*Shatrah University, Thi-Qar, 64001, Iraq*
[3]*Department of Pharmaceutical Chemistry, College of Pharmacy, University of Thi-Qar, Thi-Qar, 64001, Iraq*

[*]*Email: athraa84_chem@sci.utq.edu.iq*

Article Info
Received: July 6, 2024
Revised: July 7, 2024
Accepted: Sept 2, 2024
Online: Dec 31, 2024

Citation:
Mekky, A. H., Hamed, F. M., & Hassan, B. A. (2024). Synthesis, Characterization, Molecular Docking Studies and Pharmaceutical Evaluation of some Novel [1,2,4]Triazolo[3,4-*B*][1,3,4]Thiadiazole. *Jurnal Kimia Valensi*, 10(2), 304-314.

Doi: 10.15408/jkv.v10i2.40043

Abstract

A new series of fused [1,2,4]Triazolo[3,4-b][1,3,4]thiadiazole 4a-4e have been synthesized by many steps. Firstly, benzohydrazide [1] has been synthesized from the reaction of methyl benzoate with hydrazine hydrate. Secondly, the cyclization reaction of benzohydrazide with carbon disulfide in the presence of potassium hydroxide produced 5-phenyl-1,3,4-oxadiazole-2-thiol[2]. Thirdly,5-phenyl-1,3,4-oxadiazole-2-thiol[2] was treated with potassium hydroxide using pyridine to give 4-amino-5-phenyl-4H-1,2,4-triazole-3-thiol. Finally, the fused [1,2,4]Triazolo[3,4-*B*][1,3,4]Thiadiazole 4a-4e were synthesized from the reaction of 4-amino-5-phenyl-4H-1,2,4-triazole-3-thiol[3], with various aromatic aldehydes. The structures of the newly synthesized compounds have been confirmed based on spectral studies. The new novel compounds exhibited anticancer activity docking with C-Met tyrosin kinase receptor as shown by their docking scores ranging between -3.506 to -4.468 kcal/mol as compared to standard crizotinib binding affinity is to -3.211 kcal/mol for anticancer efficiency. The newly synthesized triazole thiadiazole derivatives were evaluated for their in-vitro cytotoxic activity against human cancer cell lines. It was found that compounds $C_{15}H_{12}N_4OS$ and $C_{15}H_{11}ClN_4S$ showed higher cytotoxicity against the MCF-7 cell line and no cytotoxic effect on normal cell line HdFn.

Keywords: Anticancer, docking, synthesis, characterization, triazolothiadiazole

1. INTRODUCTION

There has been a growing interest in active therapeutic agents in recent years. This is primarily due to the rise in metabolic diseases, the constant mutation of viral strains, the negative effects of environmental pollution on the human immune system, and the high toxicity of current medications. Consequently, synthetic chemists have been exerting significant endeavors to create novel medication candidates that demonstrate exceptional effectiveness, little harm, and maximum capacity to be absorbed by the body at a reduced expense [1]. Heterocyclic compounds, a category of these bioactive substances, play a crucial function as therapeutic agents in biological systems and are widely used in several commercial medications. The dual availability of heterocyclic compounds via natural sources and synthetic methods enhances their significance [2]. Crizotinib, a first-generation multi-target kinase inhibitor, is approved by the FDA for the treatment of ALK-positive or ROS1-positive non-small cell lung cancer (NSCLC), refractory inflammatory (ALK)-positive myofibroblastic tumors (IMTs) and relapsed /refractory ALK-positive anaplastic large cell lymphoma (ALCL). Crizotinib exists in two enantiomeric forms: (R)-crizotinib and its mirror image, (S)-crizotinib. It is assumed that the R-isomer is responsible for carrying out various processes that have been reviewed here. On the other hand, the S-isomer shows potent inhibition of MTH_1, an enzyme important for DNA repair mechanisms, Crizotinib, as shown in **Figure 1**, compared to synthesized compounds in the present study.

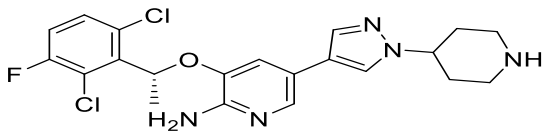

Figure 1. Chemical structure of Crizotinib

Among them, imidazole and thiadiazole derivatives are extensively studied in pharmaceutical chemistry because of their wide range of applications and diverse biological activity. The significance of imidazole and thiadiazole structures in anticancer activity lies in their biological activity, ability to interact with cellular targets, potential for selectivity, and adaptability for drug development. Moreover, their structure-activity relationship (SAR) was explored for further development [3]. The 1,3,4-thiadiazole nucleus has been used in many medicinal medications, including acetazolamide and methazolamide (which are carbonic anhydrase inhibitors used to treat glaucoma), sulfamethizole, cefazedone, cefazolin, and ceftezole (which are antibacterial treatments) [4]. In addition, a wide range of biological activities, including antibacterial, antifungal, antimicrobial, anticonvulsant, antioxidant, anti-inflammatory, antihyperlipidemic, antihypertensive, antiviral, and antisecretory, have been observed in [1,2,4]triazolo[3,4-*b*][1,3,4][3,4-*b*]thiadiazole and their derivatives. These compounds have been recognized and included in the essential medicines list.

Additionally, many compounds of [1,2,4] triazolo[3,4-*b*][1,3,4][3,4-*b*]thiadiazole is synthesized by a fused combination of two five-member heterocyclic systems of 1,2,4-triazole [5] molecules with 1,3,4-thiadiazoles. It was discovered that it has a strong ability to fight against TB [6]. Moreover, these compounds have been extensively researched in studies on anticancer activity, primarily because their structures resemble levamisole, a very effective immune system regulator [7-10].

2. RESEARCH METHODS

Materials and Instruments

The materials used were Methyl benzoate (Merck, ≥98%), Carbon disulfide (Aldrich, ≥99.9%), pyridine (Merck, ≥99.5%), N-dimethylbenzaldehyde (Aldrich, 99%), 4-hydroxybenzaldehyde (Aldrich), 4-chlorobenzaldehyde (Aldrich, 97%), 4-bromobenzaldehyde (Aldrich, 99%), 2,4-dihydroxy benzaldehyde (Aldrich, 98%), and deionized water.

Instrumentations used in this research are Fourier-transform infrared spectroscopy (FT-IR), Perkin Elmer toner 27 (Bruker, Germany), Nuclear magnetic resonance spectrometer (1H-NMR,^{13}C-NMR) BioSpin GmbH 400,100 MHz (Bruker, Germany), and Mass Spectrometer U3500(Mass Spectrometer), Mass Selective Detector(5973) (Agilent Technologies, USA).

Synthesis of benzo hydrazide [1]

A solution of hydrazine hydrate 0.5 g, 0.01 mole in 70 mL of absolute ethanol was prepared. Methyl benzoate 1.36 g, 0.01 mole, equimolar because its substitution reaction one group substituted the other good leaving group (SN_1 reaction) was added dropwise to the hydrazine solution and refluxed with stirring for 5 hours. The reaction was seen using thin-layer chromatography (TLC) using a solvent mixture of 70% hexane and 30% ethyl acetate. The solvent was evaporated slowly at a moderate temperature, resulting in the formation of a precipitate. The solid crystals were filtered, desiccated, and purified using a suitable solvent. **Table 1** presents the physical characteristics of the compounds produced [11]. The FT-IR spectra of the benzo hydrazide showed an appearance absorption band at 3247, 3137, 3084, and 1648 cm^{-1} due to stretching of NH_2, NH, ArC-H, and carbonyl of benzo hydrazide as shown in **Figure 2** [12].

Table 1. Physical properties of synthesized compounds

Comp No	Molecular formula	M.Wt	M.P °C.	Yield (%)	R_f 70% hexane 30% ethyl acetate	Color
1	$C_7H_8N_2O$	136	138-140	92	0.84	white needle
2	$C_8H_6N_2OS$	178	220-222	91	0.92	white
3	$C_8H_8N_4S$	192	189-191	90	0.66	Pink
4a	$C_{17}H_{17}N_5S$	323	261-263	73	0.71	brown
4b	$C_{15}H_{12}N_4OS$	296	267-269	75	0.75	cream
4c	$C_{15}H_{11}ClN_4S$	314	254-256	75	0.73	cream
4d	$C15H_{11}BrN4S$	359	256-258	74	0.74	brown
4e	$C_{15}H_{12}N_4O_2S$	312	258-260	75	0.73	brown

Synthesis of 5-phenyl-1,3,4-oxadiazole-2-thiol [2]

To manufacture the molecule mentioned, a quantity of 0.68 g, 0.005 moles of benzohydrazide, and 0.28 g, 0.005 mole of KOH were dissolved in 70 mL of 100% ethanol. Subsequently, the mechanism of synthesizing involves a cyclic addition reaction. The amine group of benzo hydrazide as a Nucleophile attacks the carbon disulfide in the presence of potassium hydroxide potassium to form an ionic intermediate of potassium 2-benzoylhydrazine-1-carbodithioate, cyclization occurs, a hydrogen disulfide molecule is eliminated resulting in the formation of 5-phenyl-1,3,4-oxadiazole-2-thiol, 0.4 g, 0.005 moles of CS_2 was slowly added to the mixture at a temperature of 0 °C. The combination was subjected to reflux for 72 hours until the evolution of hydrogen sulfide (H_2S) ceased. The presence of H_2S was confirmed by testing with lead acetate paper, which became black due to lead sulfide's creation. The reaction was seen using thin-layer chromatography (TLC) using a solvent mixture of 70% hexane and 30% ethyl acetate.

The solvent was evaporated and then acidified with a 10% hydrochloric acid solution. Once the reaction was finished, the mixture was transferred into crushed ice. The solid materials produced and separated were filtered and rinsed with water, then recrystallized using methanol as the solvent. The physical properties of the synthesized Compound are shown in **Table 1** [13].

Synthesis of 4-amino-5-phenyl-4*H*-1,2,4-triazole-3-thiol [3]

A solution contains a combination of two chemicals, compound 2 (1 g, 0.005 mole) and (0.28 g, 0.005 mole) of KOH, in 100 mL of pyridine. Potassium hydroxide was combined with thiol as a protective group, adding hydrazine hydrate 0.25 g, 0.005 mole. The final mixture underwent reflux for 12 hours at 250 ^{0}C. The reaction was seen using thin-layer chromatography (TLC) using a solvent mixture of 60% hexane and 40% ethyl acetate. The solvent was condensed and made acidic by adding 10% hydrochloric acid. The precipitated components were separated by filtration, rinsed with water, and then subjected to recrystallization by ethanol [14]. The physical properties of the synthesized Compound are shown in **Table 1**.

Synthesis of [1,2,4]triazolo[3,4-*b*] thiadiazole of derivatives [4a-4e]

An equimolar combination of 0.56 g, 0.01 mole of KOH, and 2 g, 0.01 mole of compound 3 was heated under reflux. Then aromatic aldehydes, N-dimethylbenzaldehyde, 4Hydroxybenzaldehyde, 4-chlorobenzaldehyde, 4-Bromobenzaldehyde, and 2,5-dihydroxybenzaldehyde 0.01 mole were added to the mixture. The resulting mixture was subjected to reflux for 8 hours. The progress of the reaction was observed using thin-layer chromatography (TLC) using a solvent combination consisting of 3 parts hexane and seven parts ethyl acetate. The solvent was condensed, and the liquid was cooled before being placed over crushed ice while agitated. The solid obtained was separated by filtration and then recrystallized using acetone as the solvent [15-18]. The physical properties of the synthesized Compound are listed in **Table 1**, as shown in **scheme 1**.

The FT-IR spectrum of **4a Figure 2** exhibited the appearance of new band absorption 3106 cm^{-1} of NH, 3078 cm^{-1} of Ar C-H, 2990 cm^{-1} of AliC-H,1691 cm^{-1} of C=N of triazole ring and 558 cm^{-1} of C-N. The ^{1}H-NMR spectrum of Compound **4a Figure 3** showed singlet signals for NH proton at δ14.14 ppm and multiplate signals at 7.83 (m, 2H, ArC-H), 7.70 (s, 2H, ArC-H), 7.68 (s, 2H, ArC-H), 7.59 – 7.46 (m, 3H, ArC-H) 6.77 of (s,1H, CH) and 3.01 (s, 6H, N(CH_3). The ^{13}C-NMR spectrum of compounds **4a Figure 4** revealed signals at 165.02,161.14 ppm correspond to (C=N-NH),(C=N-Ar) of triazole ring, 148.81ppm of Ar-N(CH_3)2and 131.02, 130.03, 129.16, 128.62, 126.13, 110.24, 109.17 ppm of aromatic carbon and 102.84 ppm of CH. The mass spectrum 4a **Figure 5** showed a molecular ion peak at 323 of $[C_{17}H_{17}N_5S]^{+,}$ and 146 corresponded to the basic peak [19].

The FT-IR spectrum of **4b Figure 6** exhibited the appearance of band 3455 cm^{-1} corresponding to stretching vibration of OH and the appearance of new band absorption at 3135 cm^{-1} of NH, 3065 cm^{-1} of ArC-H, 2972 cm^{-1} of AliC-H,1674 cm^{-1} of C=N of triazole ring and 547 cm^{-1} of C-OH. The ^{1}H-NMR spectrum of Compound **4b Figure 7** displayed the following signals δ(ppm)14.19 (s, 1H, NH), 10.43 (s, 1H, OH),8.02 – 7.79 (m, 2H, Aromatic protons), 7.76 (d, J = 8.6 Hz, 2H, Aromatic protons), 7.70 (d, J = 8.6 Hz, 2H, Aromatic protons), 7.53 (s, 1H, Aromatic protons), 6.42 (s, 1H, CH). The ^{13}C-NMR spectrum of compounds **4b Figure 8** showed signals at 163.74, 159.04 ppm corresponding to C=N-NH, C=N-Ar of triazole ring, 149.07ppm of Ar-OH carbon and signals at 134.94, 133.71, 131.09, 128.77, 127.72, 126.03, 120.07, 118 ppm of aromatic carbon and 116.99 of CH carbon. Mass spectra of 4b showed molecular ion peak at 296 of $[C_{15}H_{12}N_4OS]^+$ and 177 corresponded to the basic peak in **Figure 9**.

The FT-IR spectrum of **4c Figure 10** displayed the appearance band 3138 cm^{-1}correspond to new band absorption of NH, 3065 cm^{-1} of ArC-H, 2999 cm^{-1} of AliC-H,1649 cm^{-1} of C=N of triazole ring and 561 cm^{-1} of C-Cl. The ^{1}H-NMR spectrum of Compound 4c **Figure 11** showed signals (ppm): δ13.95 (s, 1H, NH), 8.26 – 8.11 (m, 1H, Ar), 8.07 – 7.98 (m, 2H, Ar), 7.88 (d, J = 7.4 Hz, 2H, Ar), 7.62 – 7.53 (m, 4H, Ar), 7.38 (m, 1H, Ar) and 6.64 of (s, 1H,

CH). The ^{13}C-NMR spectrum of Compound **4c Figure 12** showed signals at 166.29.04 ppm and 165.73ppm, corresponding to C=N-NH, C=N-Ar of triazole ring, 151.11ppm of Ar-Cl while signals at 133.56, 133.01, 132.33, 129.51, 129.30, 128.97, 128.09, 127.93, 127.73 ppm refer to aromatic carbon, on the other hand signal at 109.84 ppm due to CH. The mass spectrum **4c Figure 13** showed a molecular ion peak at 314 of [$C_{15}H_{11}ClN_4S$], and 177 corresponded to the basic peak.

The FT-IR spectrum of **4d Figure 14** showed appearance band absorption at 3149 cm^{-1} refer to stretching vibration of NH, 3036 cm^{-1} of ArC-H, 2936 cm^{-1} of AliC-H, 1608 cm^{-1} of C=N of triazole ring and 593 cm^{-1} of C-Br. ^{1}H NMR (400 MHz, DMSO-d_6) spectrum of Compound **4d Figure 15** exhibits the following signals: 7.87 (d, J = 3.0 Hz, 2H), 7.82 – 7.52 (m, 4H), 7.52 (dd, J = 5.3, 1.1 Hz, 3H), 6.80 (s, 1H, CH). The FT-IR spectrum of **4e Figure 16** showed the appearance of new band absorption at 3549 cm^{-1} of OH, 3100 cm^{-1} of NH, 3044 cm^{-1} of ArC-H, 2925 cm^{-1} of AliC-H,1691 cm^{-1} of C=N of triazole ring and 511 cm^{-1} of C-OH. The ^{1}H-NMR spectrum of compounds **4e Figure 17** displayed signals for (NH), OH, OH at 14.21 (s, 1H, NH), 11.15 (s, 1H, OH), 10.50 (s, 1H, OH), 7.91 – 7.84 (m, 2H, Ar C-H), 7.69 (d, J= 7.1 Hz, 1H ArC-H), 7.53 (s, 3H, Ar C-H), 7.42 (dt, J = 15.3, 7.2 Hz, 2H, ArC-H), 6.92 (s, 1H). 6.77 of (s, 1H, CH) [20-28].

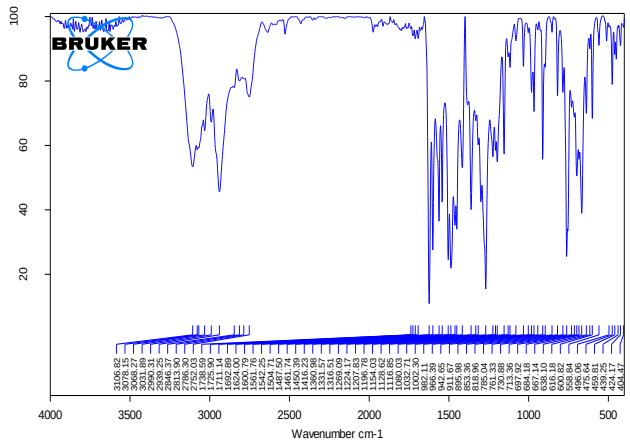

Figure 2. FT-IR Spectrum of Compound 4a.

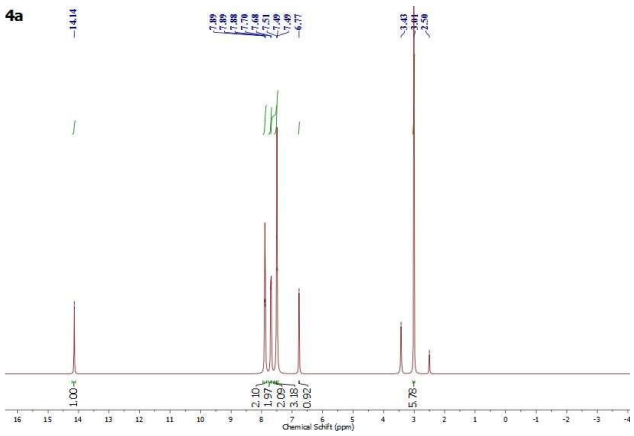

Figure 3. ^{1}H-NMR Spectrum of Compound 4a

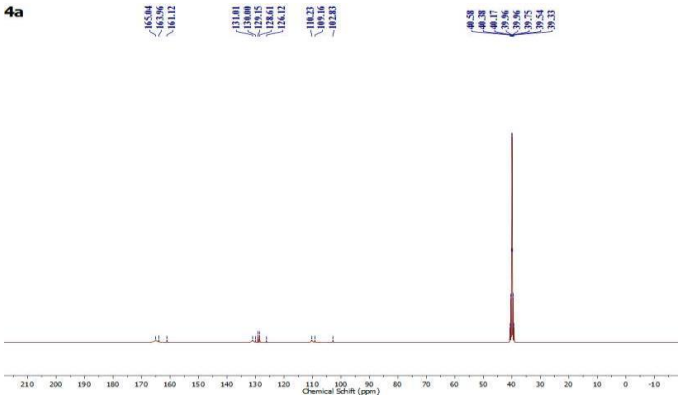

Figure 4. ^{13}C-NMR Spectrum of Compound 4a

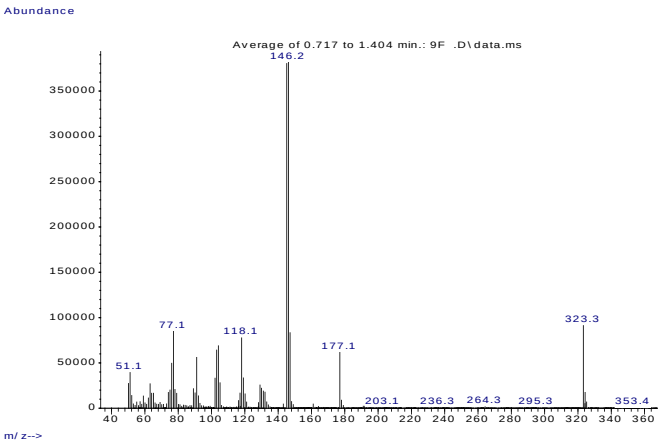

Figure 5. Mass Spectrum of Compound 4a

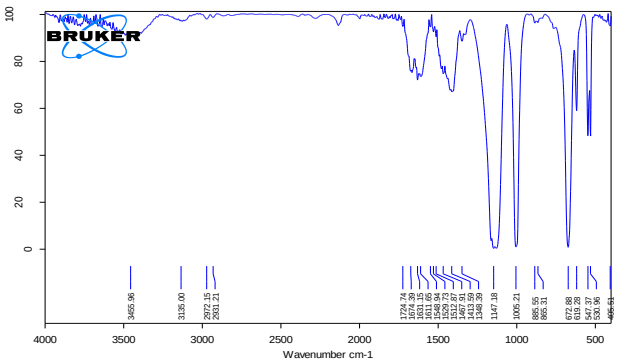

Figure 6. FT-IR Spectrum of Compound 4b

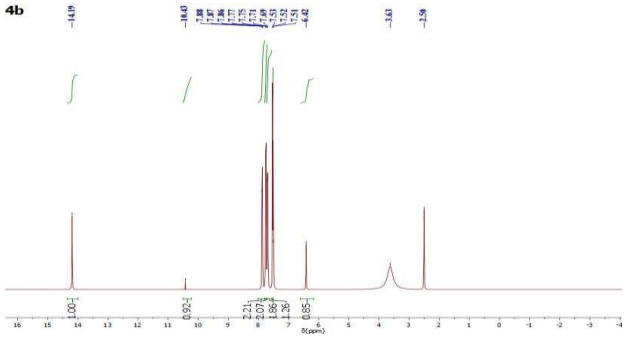

Figure 7. ^{1}H-NMR Spectrum of Compound 4b

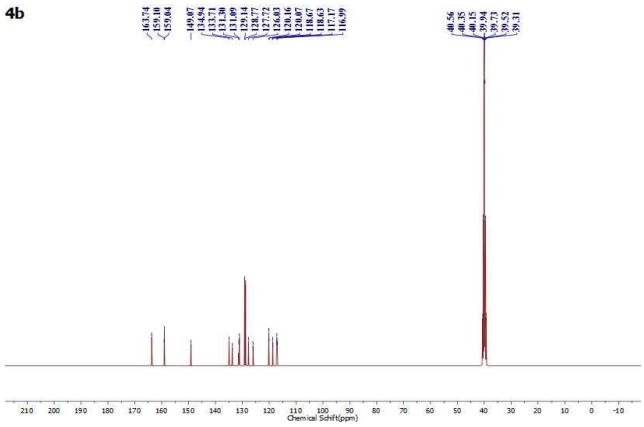

Figure 8. ^{13}C-NMR Spectrum of Compound 4b

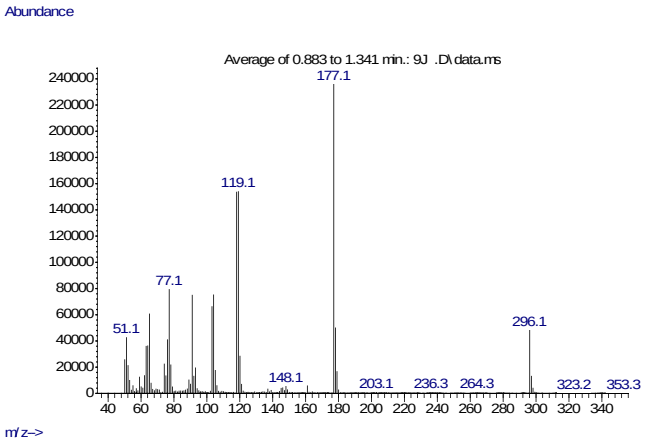

Figure 9. Mass Spectrum of Compound 4b

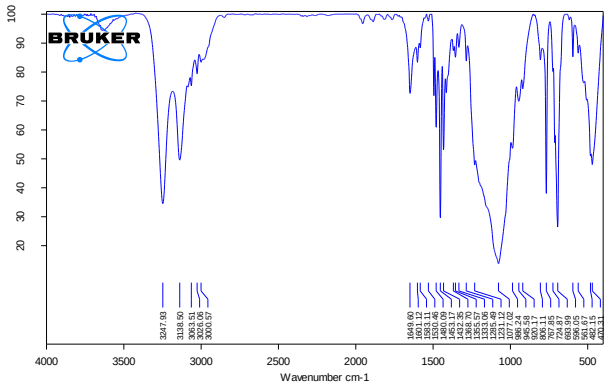

Figure 10. FT-IR Spectrum of Compound 4c

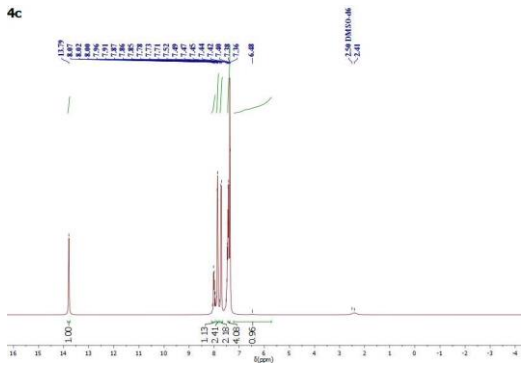

Figure 11. ^{1}H-NMR Spectrum of Compound 4c

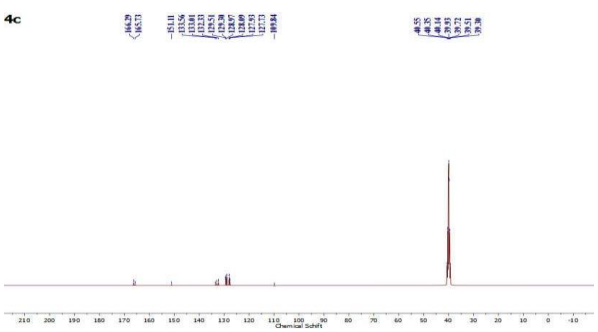

Figure 12. ^{13}C-NMR Spectrum of Compound 4c

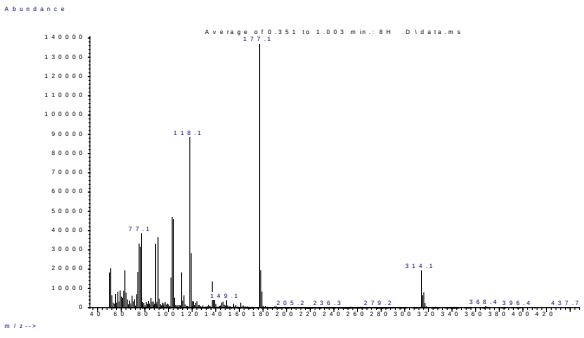

Figure 13. Mass Spectrum of Compound 4c

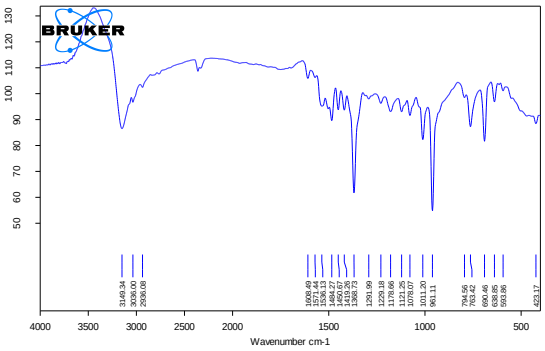

Figure 14. FT-IR Spectrum of Compound 4d

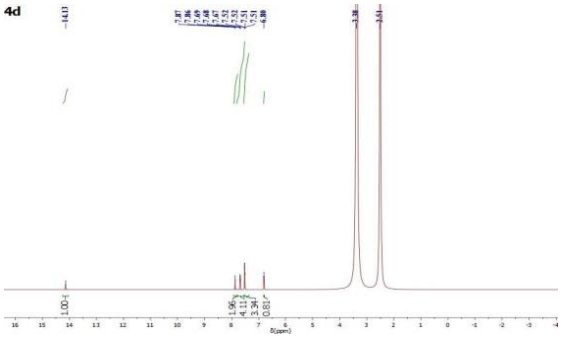

Figure 15. ^{1}H-NMR Spectrum of Compound 4d

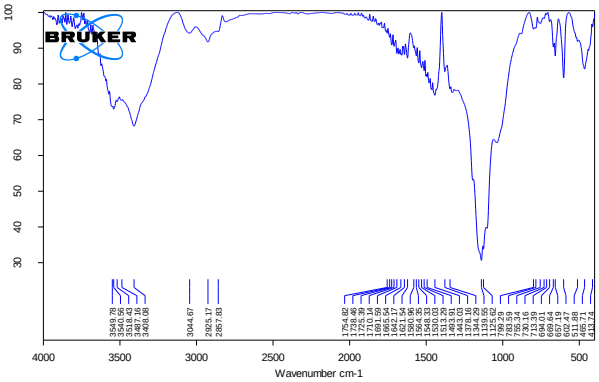

Figure 16. FT-IR Spectrum of Compound 4e

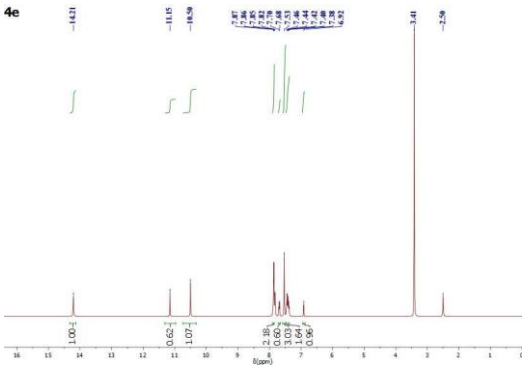

Figure 17. 1H-NMR Spectrum of Compound 4e

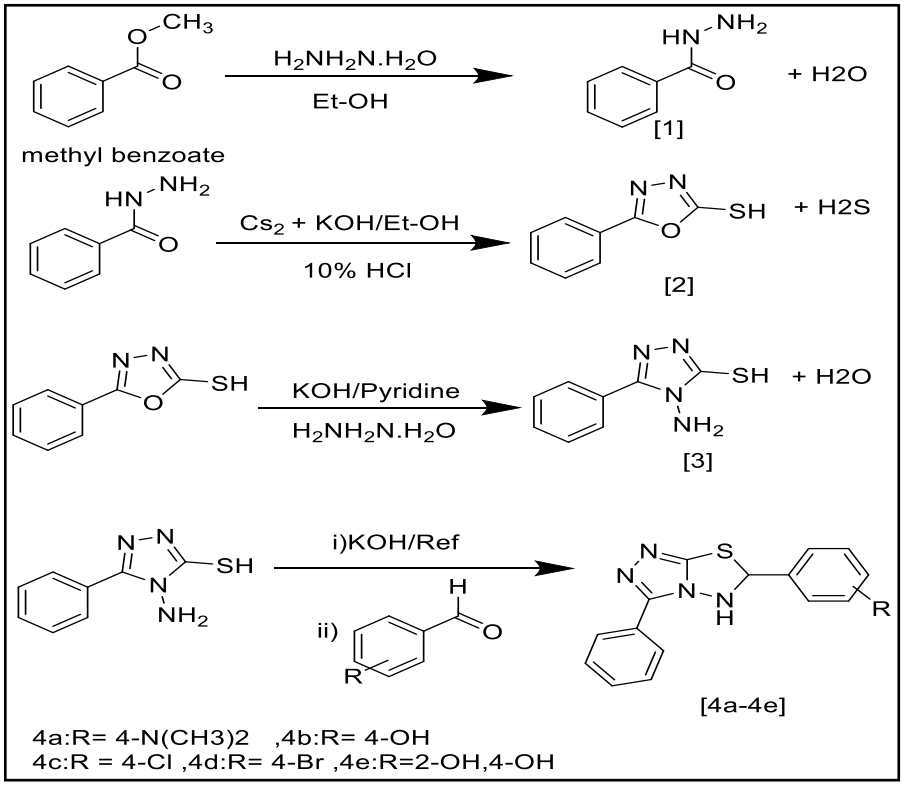

Scheme 1. Synthesis of Novel [1,2,4]Triazolo[3,4-*b*][1,3,4]Thiadiazole[4a-4e]

3. RESULTS AND DISCUSSION

According to the previous results, the study concluded that the synthesized target compounds had been successfully done. The purity and characterization of the synthesized compounds were confirmed by determining their physical properties, such as melting point, R_f values, FT-IR spectrum,^{1}H-NMR,^{13}C-NMR, and Mass spectra. The preliminary cytotoxicity evaluation of some of the synthesized final compounds **4b, 4c** on MCF-7 Showed that these compounds have a highly cytotoxic effect represented by their high inhibitory percent and may represent an exploitable source of new anticancer agents. Comparative cytotoxic study compounds **4b 4c** are the best and most selective agents because of their low toxicity to the normal cells HdFn with higher toxicity to the cancer cells with MCF-7. It may represent an exploitable source of new anticancer agents.

Molecular docking study

The newly synthesized chemicals had an anticancer impact, as shown by the molecular docking investigation. The drugs exhibit anticancer effects by targeting the C-Met tyrosine kinase receptor with varying degrees of efficacy. Their docking scores vary between -4.468 and -3.506 kcal/mol, whereas the binding affinity of Crizotinib is -3.211 kcal/mol. Furthermore, Compound **4b** exhibited the most significant binding affinity with a -4.468 kcal/mol value. When these chemicals are placed into the C-Met tyrosine kinase receptor, they exhibit anticancer action with varying binding affinity, as shown in **Table 2**. Hydrogen bonds (H-bonds) are established with amino acid residues in the active site of the protein receptor, along with other brief contacts that strengthen the connection (30,31). The molecule **4b** has a docking score of -4.468 kcal/mol and is bound by one hydrogen bond with ASP 123, as illustrated **in Figure 18**.

Compound **4c** had a docking score of -3.55 Kcal/mol, indicating its strong binding to the receptor. One hydrogen bond with GLY 79 and one salt bridge with ARG 73 facilitates this binding, as seen in **Figure 19**. The Compound **4d** had a docking score of -3.506 kcal/mol, indicating its strong binding to the receptor. One hydrogen bond with GLY 79 and one salt bridge with ARG 73 facilitates this binding, as seen in **Figure 20**. The Crizotinib drug.had a docking score of -3.211 Kcal/mol, indicating It formed a single hydrogen bond with THR 75, as shown in **Figure 21,** as illustrated in **Table 2** [29-30].

Table 2. Results of molecular interaction between c-met tyrosine inhibitor, compounds **4b,4c,4d**, and reference Crizotinib drug

Title	Docking score on ER – (Kcal/mol)	H-bond	Others bonds
4b	-4.468	ASP 123	--
4c	-3.55	THE 75	--
4d	-3.506	GLY 79	Salt bridge with ARG 73
Crizotinib drug	-3.211	ASP 123, ASN 77	Salt bridge with ASP 123

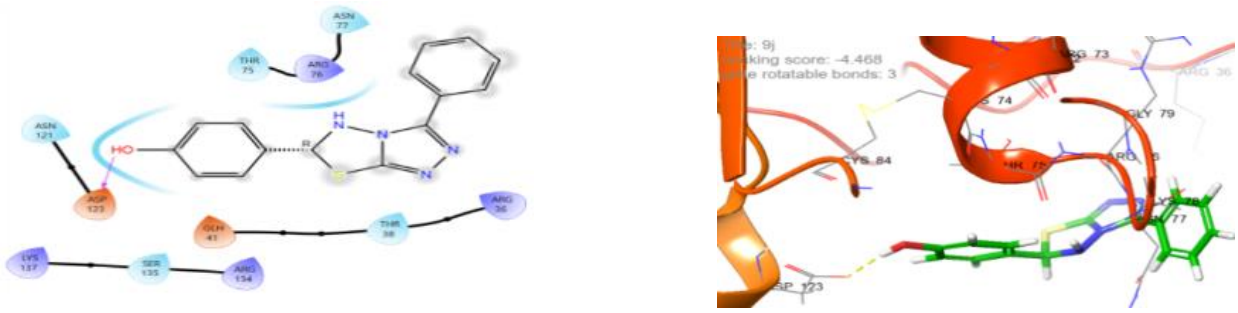

2D 3D

Figure 18. 2D and 3D dimensional representations of molecular interactions between c-met tyrosine inhibitor and

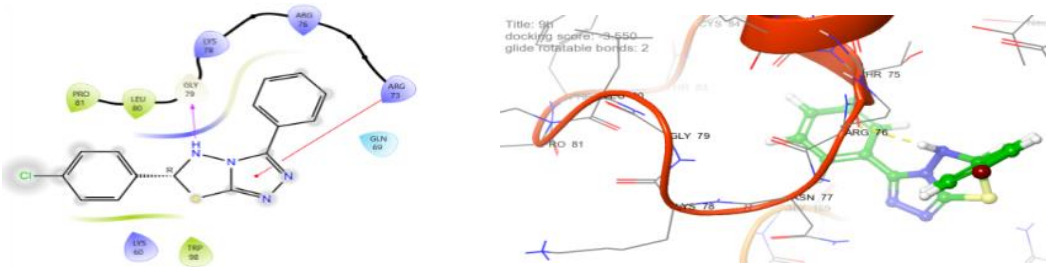

2D 3D

Figure 19. 2D and 3D dimensional representations of molecular interactions between c-met tyrosine inhibitor and **4c** Compound

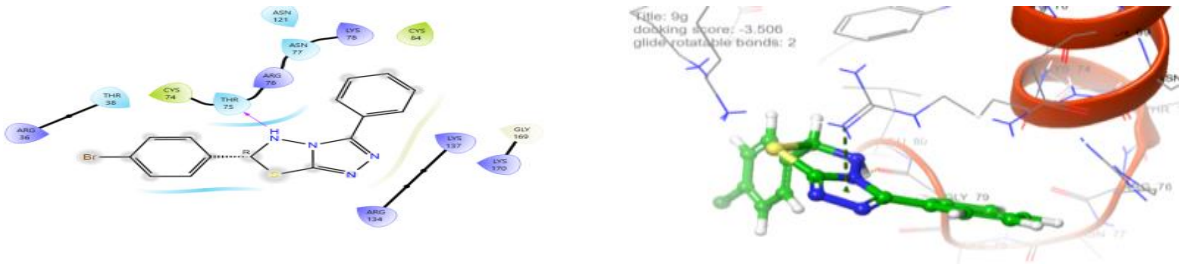

2D 3D

Figure 20. 2D and 3D dimensional representations of molecular interactions between c-met tyrosine inhibitor and **4D** Compound

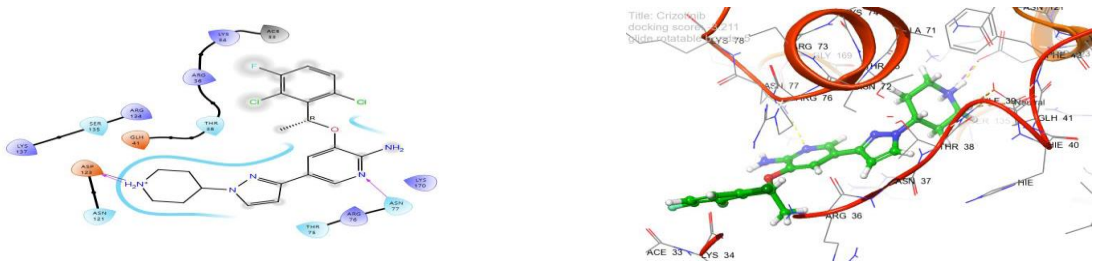

2D 3D

Figure 21. 2D and 3D dimensional representations of molecular interactions between c-met tyrosine inhibitor and Crizotinib drug.

Cytotoxicity screening

The synthesized compounds **4b and 4c** were evaluated for their cytotoxicity against MCF-7 and HdFn cell lines using the MTT assay. This assay is based on the color change of (3-(4,5-dimethyl-2-thiazolyl)bromide-2,5-diphenyl-2H-tetrazolium) from yellow to purple when live cells undergo apoptosis. After incubating the plates at body temperature and in the presence of CO_2 for 24 hours, various concentrations (25, 50, 100, 200, and 400 µg mL^{-1}) of the synthesized compounds **4b, 4c** were added. The results of IC_{50}, which represents the half maximal inhibitory concentration, indicated that the synthesized compounds **4b and 4c** exhibit anticancer activity. However, the activity level varies depending on the function—substitution group of the compounds. Furthermore, the effectiveness of the anticancer activity is directly proportional to the concentration of the drugs used, with low concentrations showing minimal effectiveness. Additionally, the lipophilicity and van der Waals volume are crucial considerations. The synthesized chemicals **4b and 4c** exhibited significant cytotoxicity against the MCF-7 cell line at 111.7µg/mL and 96.32 µg/mL concentrations. However, low cytotoxic impact on the human normal cell line (HdFn Cell line) at 230.2 µg/mL concentrations and 171.8 µg/mL, respectively, are illustrated in **Figures 22, Tables 3 and 4** [31-33].

Table 3. Cytotoxic effects of 4a at different concentrations on MCF-7 and HdFn

4b	HdFn		MCF-7	
Conc. µg/mL	mean	SD	mean	SD
400	75.268	1.300019	41.509	4.454175
200	86.53233	1.214645	49.64967	5.1057718
100	83.75	0.405962	67.50633	1.762863
50	90.56	0.900286	78.16033	0.937438
25	91.872	0.951826	88.30733	3.45387

Table 4. Cytotoxic effects of 3c at different concentrations on MCF-7 and HdFn

4c	HdFn		MCF-7	
Conc. µg/mL	mean	SD	mean	SD
400	75.267	1.201014	51.509	6.254159
200	88.53233	1.415646	56.64967	4.957719
100	96.75	0.405963	70.50633	2.562853
50	90.56	0.910287	84.16033	1.837451
25	92.872	0.501827	97.30733	4.25387

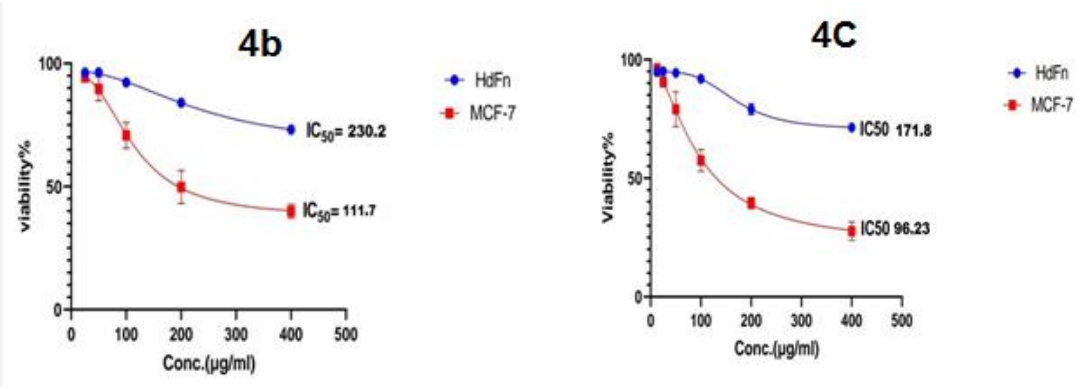

Figure 22. Dose-dependent cytotoxic effect of **4b, 4c** on MCF-7 and HdFn cell lines

CONCLUSION

In this study, [1,2,4]triazolo[4,3-b][1,2,4,5] thiadiazole derivatives **4a-4e** were synthesized via cyclization reaction. The synthesized compounds were confirmed by some spectral methods such as FTIR, ^{1}H-NMR, and ^{13}C-NMR. The newly synthesized compounds exhibited an anticancer effect When docked inside the C-Met tyrosin kinase receptor, as shown by their docking scores ranging from -6.058 to -4.853 kcal/mol. In contrast, Crizotinib binding affinity is -3.506 to -4.468 Kcal/mol. It showed the highly cytotoxic effect of the synthesized Compound on the MCF-7 Cell line (µg/mL). They synthesized compounds that showed no cytotoxic effect on human normal Cells (HdFn Cell line). The molecular docking results showed consistency with in vitro laboratory results, and it is possible to exploit these new compounds as new cancer agents.

ACKNOWLEDGMENTS

The College of Pharmacy, Thiqar University, and the Ministry of Higher Education and Scientific Research, Iraq, supported this study.

REFERENCES

1. Banerjee A, Kundu S, Bhattacharyya A, Sahu S, Maji MS. Benzannulation strategies for the synthesis of carbazoles, indolocarbazoles, benzocarbazoles, and carbolines. Organic Chemistry Frontiers. 2021;8(11):2710-71. https://doi.org/10.1039/D1QO00092F
2. Stetsiuk O, Abhervé A, Avarvari N. 1, 2, 4, 5-Tetrazine-based ligands and complexes. Dalton Transactions. 2020;49(18):5759-77. https://doi.org/10.1039/D0DT00827C.
3. Reza Emamali S, Abbas N, Yaser N, Morteza B, Karim A, Naser S. Synthesis and determination of stability constants of a new bis-1, 2, 4-triazole ligand for complexation with zinc (II), copper (II) and nickel (II) in acetonitrile. American Journal of Analytical Chemistry. 2012 Jun 21;2012. http://dx.doi.org/10.4236/ajac.2012.36057.
4. Hassan BA, Mekky AH. Synthesis, molecular docking, and anticancer study of some new [1, 2, 4] triazolo [4, 3-b][1, 2, 4, 5] tetrazines. Indian Journal of Heterocyclic Chemistry. 2024 Jul;34(03):391-8. https://doi.org/10.59467/IJHC.2024.34.391.
5. Hassan BA, Hamed FM. Synthesis and Pharmaceutical Activity Of Triazole Schiff Bases With Theoretical Characterization. Kimya ProblemLeri. 2024;22(3):332-41. DOI: 10.32737/2221-8688-2024-3-332-341
6. Hassan, b.a., meekly, a.h.synthesis, characterization and antibacterial activity of [1,2,4]triazolo[4,3-b][1,2,4,5]tetrazine derivatives, chemical problems, 2025, 23(1), pp. 78–94, https://DOI:10.32737/2221-8688-2025-1-78-94
7. Sharma K, Porat ZE, Gedanken A. Designing natural polymer-based capsules and spheres for biomedical applications—a review. Polymers. 2021 Dec 9;13(24):4307. https://doi.org/10.3390/polym13244307.
8. Li X, Liu Y, Yu Y, Chen W, Liu Y, Yu H. Nanoformulations of quercetin and cellulose nanofibers as healthcare supplements with sustained antioxidant activity. Carbohydrate polymers. 2019 Mar 1;207:160-8. https://doi.org/10.1016/j.carbpol.2018.11.084
9. Adepu S, Ramakrishna S. Controlled drug delivery systems: current status and future directions. Molecules. 2021 Sep 29;26(19):5905.https://doi.org/10.3390/molecules26195905
10. Liauw CM, Vaidya M, Slate AJ, Hickey NA, Ryder S, Martínez-Periñán E, McBain AJ, Banks CE, Whitehead KA. Analysis of cellular damage from bacteria exposure to graphene oxide and hybrids using Fourier transform infrared spectroscopy. Antibiotics. 2023 Apr 18;12(4):776.https://doi.org/10.3390/antibiotics12040776
11. Fan Y, Lu YM, Yu B, Tan CP, Cui B. Extraction and purification of capsaicin from capsicum oleoresin using an aqueous two-phase system combined with chromatography. Journal of Chromatography B. 2017 Sep 15;1063:11-7. https://doi.org/10.1016/j.jchromb.2017.07.006
12. Abdulridha, M.M., Abdulhussein, H.S., Alyaseen, F.F., Hassan, B.A. Phytochemical and antibacterial activity of the bignum harmalaseeds and its alkaloids. Plant Archives, 2019, 19(1), pp. 1439–1444. http://www.plantarchives.org/PDF%2019-1/1439-1444%20(4739).pdf
13. Rosspertiwi R, Yunus AL, Rahayu DP. Farah Nurlidar, & Azizah, YN. Synthesis and Characterization of Low Molecular Weight Irradiated Chitosan in Various Water Levels and Gamma-Ray Doses. Jurnal Kimia Valensi. 2024 Jun 9;10(1):115-22. https://doi.org/10.15408/jkv.v10i1.36509.
14. wibowo hb. pengembangan teknik analisis berat molekul htpb untuk acuan dalam kontrol kualitas. jurnal teknologi dirgantara. 2018 sep 17;16(1):59-70. http://dx.doi.org/10.30536/j.jtd.2018.v16.a2871
15. Li Y, Wu C, Wu T, Yuan C, Hu Y. Antioxidant and antibacterial properties of coating with chitosan–citrus essential oil and effect on the quality of Pacific mackerel during chilled storage. Food science & nutrition. 2019 Mar;7(3):1131-43. https://doi.org/10.1002/fsn3.958.
16. Gryczka U, Dondi D, Chmielewski AG, Migdal W, Buttafava A, Faucitano A. The mechanism of chitosan degradation by gamma and e-beam irradiation. Radiation Physics and Chemistry. 2009 Jul 1;78(7-8):543-8.https://doi.org/10.1016/j.radphyschem.2009.03.081.
17. Martini M, Saraswati LD, Dirgantara RC. Pengaruh Variasi Kepadatan Pupa Aedes Aegypti Jantan dalam Media Radiasi Sinar Gamma 70 Gy terhadap Tingkat Kemunculan Dewasa. Jurnal Kesehatan Masyarakat Universitas Diponegoro. 2016;4(1):18527.http://ejournal-s1.undip.ac.id/index.php/jkm.
18. Cheng J, Zhu H, Huang J, Zhao J, Yan B, Ma S, Zhang H, Fan D. The physicochemical properties of chitosan prepared by microwave heating. Food Science & Nutrition. 2020 Apr;8(4):1987-94. https://doi.org/10.1002/fsn3.1486.

19. Mulyani R, Mulyadi D, Yusuf N. Preparation and characterization of chitosan membranes from crab shells (Scylla olivacea) for beverage preservative. Jurnal Kimia Valensi. 2019 Nov 30;5(2):242-7. http://dx.doi.org/10.15408/jkv.v5i2.10637.
20. Rosspertiwi R, Yunus AL, Rahayu DP. Farah Nurlidar, & Azizah, YN (2024). Synthesis and Characterization of Low Molecular Weight Irradiated Chitosan in Various Water Levels and Gamma-Ray Doses. Jurnal Kimia Valensi. 2024 Jun 9;10(1):115-22. https://doi.org/10.15408/jkv.v10i1.36509.
21. Ruswanto R, Rahayuningsih N, Hidayati NL, Nuryani GS, Mardianingrum R. Uji In Vitro dan Studi In Silico Senyawa Turunan n'-benzoylisonicotinohydr. Jurnal ILmu Kefarmasian Indonesia. 2019 Oct 29;17(2):218-26. https://doi.org/10.35814/jifi.v17i2.703.
22. Vinsiah R, Fadhillah F. Studi Ikatan Hidrogen Sistem Metanol-Metanol dan Etanol-Etanol dengan Metode Molekular Dinamik. Sainmatika: Jurnal Ilmiah Matematika dan Ilmu Pengetahuan Alam. 2018 Jun 5;15(1):14-22. https://doi.org/10.31851/sainmatika.v15i1.1739
23. Prayoga H. Analisis Dinamika Molekul Protein Lysozyme Putih Telur Dengan Model Potensial Lennard-Jones Menggunakan Aplikasi Gromacs. http://digilib.unila.ac.id/id/eprint/57470.
24. Esmaeili H, Foroutan R. Adsorptive Behavior of Methylene Blue onto Sawdust of Sour Lemon, Date Palm, and Eucalyptus as Agricultural Wastes. Journal of Dispersion Science and Technology. 2019;40(7):990-999. https://doi.org/10.1080/01932691.2018.1489828
25. Hollup SM, Fuglebakk E, Taylor WR, Reuter N. Exploring the factors determining the dynamics of different protein folds. Protein Science. 2011 Jan;20(1):197-209.https://doi.org/10.1002/pro.558
26. Yin C, Feng L, Zhang N, Cheng Y. How environmental factors affect the structural properties and biofunctions of keratin: a molecular dynamics study. Materials Today Communications. 2023 Mar 1;34:105254.https://doi.org/10.1016/j.mtcomm.2022.105254
27. Hamed FM, Hassan BA, Abdulridha MM. The antitumor activity of sulfonamide derivatives. Int. J. Pharm. Res. 2020 Jun;12:2512-9.http://dx.doi.org/10.13140/RG.2.2.10866.07369
28. Rosanti AD, Kusumawati Y, HiDayat F, Fadlan A, Wardani AR k., Anggraeni HA. Adsorption of Methylene Blue and Methyl Orange from Aqueous Solution using Orange Peel and CTAB-Modified Orange Peel. Journal of the Turkish Chemical Society Section A: Chemistry. 2022;9(1):237-246. https://doi.org/10.18596/jotcsa.1003132
29. Shalaal SH, Halail AT, Hamed FM, Hassan BA. Maceration techniques extraction of thymus vulgaris and laurel (Laurus Nobilis) Leaves with antibacterial study. Plant Archives. 2019;19(2):4041-4. http://www.plantarchives.org/19-2/4041-4044%20(5943).pdf
30. Abass AA, Muhsin SN, Hasan SA, Hassan BA. Efficacy study of Captopril on some liver function tests in hypertensive patients. Revista Latinoamericana de Hipertension. 2023 Jul 1;18(3):142-6. https://doi.org/10.5281/zenodo.8052329.
31. Fang J, Gao B, Mosa A, Zhan L. Chemical activation of hickory and peanut hull hydrochars removes lead and methylene blue from aqueous solutions. Chemical Speciation & Bioavailability. 2017;29(1):197-204. https://doi.org/10.1080/09542299.2017.1403294
32. Hassan, B.A., Baqer, F.M., Abdulridha, M.M.. Design, synthesis, and characterization of benzoxazepine thiourea new derivatives. International Journal of Drug Delivery Technology. 2021, 11(3), pp. 874–876. DOI: 10.25258/ijddt.11.3.37
33. Shalaal, S.H., Halail, A.T., Hamed, F.M., Hassan, B.A. Maceration techniques extraction of Thymus vulgaris and laurel (Laurus nobilis) leaves with antibacterial study, Plant Archives, 2019, 19(2), pp. 4041–4044.DOI: 10.13140/RG.2.2.32388.55688